• *Original Paper* •

Characterization of Organic Aerosol at a Rural Site in the North China Plain Region: Sources, Volatility and Organonitrates

Qiao ZHU[1,2], Li-Ming CAO[1], Meng-Xue TANG[1], Xiao-Feng HUANG[1],
Eri SAIKAWA[2,3], and Ling-Yan HE[*1]

[1]*Key Laboratory for Urban Habitat Environmental Science and Technology*,
Peking University Shenzhen Graduate School, *Shenzhen* 518055, *China*
[2]*Department of Environmental Sciences*, *Emory University*, *Atlanta*, *GA* 30322, *USA*
[3]*Rollins School of Public Health*, *Emory University*, *Atlanta*, *GA* 30322, *USA*

ABSTRACT

The North China Plain (NCP) is a region that experiences serious aerosol pollution. A number of studies have focused on aerosol pollution in urban areas in the NCP region; however, research on characterizing aerosols in rural NCP areas is comparatively limited. In this study, we deployed a TD-HR-AMS (thermodenuder high-resolution aerosol mass spectrometer) system at a rural site in the NCP region in summer 2013 to characterize the chemical compositions and volatility of submicron aerosols (PM_1). The average PM_1 mass concentration was 51.2 ± 48.0 μg m^{-3} and organic aerosol (OA) contributed most (35.4%) to PM_1. Positive matrix factorization (PMF) analysis of OA measurements identified four OA factors, including hydrocarbon-like OA (HOA, accounting for 18.4%), biomass burning OA (BBOA, 29.4%), less-oxidized oxygenated OA (LO-OOA, 30.8%) and more-oxidized oxygenated OA (MO-OOA, 21.4%). The volatility sequence of the OA factors was HOA > BBOA > LO-OOA > MO-OOA, consistent with their oxygen-to-carbon (O:C) ratios. Additionally, the mean concentration of organonitrates (ON) was 1.48−3.39 μg m^{-3}, contributing 8.1%−19% of OA based on cross validation of two estimation methods with the high-resolution time-of-flight aerosol mass spectrometer (HR-ToF-AMS) measurement. Correlation analysis shows that ON were more correlated with BBOA and black carbon emitted from biomass burning but poorly correlated with LO-OOA. Also, volatility analysis for ON further confirmed that particulate ON formation might be closely associated with primary emissions in rural NCP areas.

Key words: organic aerosols, volatility, organonitrates, biomass burning, North China Plain

Article Highlights:

- Four types of OA factors were resolved by PMF at a rural NCP site. The volatility sequence of OA factors was consistent with their O:C ratios.
- Organonitrates evaporated faster than OA factors but slower than inorganic nitrates, suggesting they were more relevant to primary emissions.
- Organonitrates accounted for 8.1%−19% of OA and they were largely influenced by biomass burning emissions in rural NCP areas.

---

1. Introduction

Atmospheric fine aerosols have attracted much attention from the public owing to their adverse effects on visibility, global climate and human health (Dockery et al., 1993; Charlson and Heintzenberg, 1995; Haywood and Boucher, 2000; Ramanathan et al., 2001; IPCC, 2013). The North China Plain (NCP), which is one of the most important city clusters in China, is a global hotspot of aerosol pollution originated from both natural (e.g., dust storms) and anthropogenic (e.g., industrial emissions, vehicle emissions and biomass burning) sources. As a result, numerous studies on the sources, formation and evolution processes of aerosols have been conducted in urban regions, such as Beijing, Tianjin, and some cities in Hebei Province that have experienced

---

* Corresponding author: Ling-Yan HE
  Email: hely@pku.edu.cn

severe air pollution (Song et al., 2006; Gu et al., 2010; Huang et al., 2010; Liu et al., 2012; Sun et al., 2012; Wang et al., 2014; Li et al., 2017). Compared to studies on the urban atmosphere, studies focusing on aerosol characterization in rural NCP areas are much more limited. For example, as a key property for aerosols, volatility can greatly influence the mass concentration and size distribution of aerosols via gas–particle partitioning (Lazaridis, 1999; Pankow and Barsanti, 2009; Bilde et al., 2015), and previous studies suggest that the volatility of different aerosol compounds may vary from site to site (Huffman et al., 2009a, b; Bi et al., 2015; Cao et al., 2018, 2019; Xu et al., 2019). However, to the best of our knowledge, aerosol volatility measurements in rural NCP areas do not exist. Research on the volatility of different aerosol compounds in rural NCP areas is needed to obtain a more comprehensive understanding of aerosol fate on the regional scale. Three methods are frequently applied to measure the volatility of aerosols: VTDMA (volatility tandem differential mobility analyzer) (Dassios and Pandis, 1999; Kuhn et al., 2005; Saleh et al., 2008), dilution samplers (Shrivastava et al., 2006), and the combination of a thermodenuder and aerosol mass spectrometer (TD-AMS system) (Huffman et al., 2008). Among them, the TD-AMS system can measure the volatility of different chemical compositions with a high temporal resolution and has been widely used in field campaigns (Huffman et al., 2009a, b; Bi et al., 2015; Cao et al., 2018, 2019; Xu et al., 2019) and laboratory studies (Kolesar et al., 2015; Saha and Grieshop, 2016).

Organonitrates (ON) are generating increasing interest owing to their crucial role in the chemistry of atmospheric oxidation and potentially significant influence on regional air quality, climate change and global biogeochemical cycles (Bertman et al., 1995; Jenkin and Clemitshaw, 2000; Russo et al., 2010). The broad definition of ON includes peroxy nitrates (RO_2NO_2) and multifunction alkyl nitrates ($RONO_2$). Lacking the ideal analytical instruments to detect the bulk ON was the biggest obstacle for fully understanding the chemistry of ON in the past. In recent years, several advanced techniques have emerged that are capable of measuring various kinds of ON, especially for particulate ON. Aerosol mass spectrometry (AMS), which has been widely used to characterize organic compounds of aerosols with high temporal resolution, can quantify the number of ON species based on indirect estimation methods (Farmer et al., 2010; Hao et al., 2014; Xu et al., 2015a, b). Rollins et al. (2012) reported the first direct ambient measurement of particulate ON by the Berkeley thermal dissociation-laser induced fluorescence method. These measurements provided significant evidence that ON contribute a substantial portion of the secondary organic aerosols (Rollins et al., 2012; Fry et al., 2013; Ayres et al., 2015; Boyd et al., 2015; Xu et al., 2015b; Lee et al., 2016; Yu et al., 2019). There are two main secondary formation pathways for ON: OH-initiated oxidation of hydrocarbons in the presence of NO_x in the daytime, and NO_3-induced oxidation of alkenes at night. For

the secondary formation pathway, several studies have shown that particulate ON yields were high via nighttime NO_3 reacting with biogenic unsaturated alkenes (i.e., isoprene and monoterpene) (Fry et al., 2009; Ayres et al., 2015; Boyd et al., 2015, 2017). Very recently, Joo et al. (2019) reported that particulate ON can be formed from the reaction of NO_3 oxidation of 3-Methylfuran, which is an important tracer species in biomass burning plumes. However, the properties, sources and formation mechanisms of particulate ON are still not well understood (Perring et al., 2013). To the best of our knowledge, most research on particulate ON has been conducted in the U.S. and Europe (Perring et al., 2013; Ng et al., 2017), and very few studies have reported detailed particulate ON results for urban areas in China (Xu et al., 2017; Yu et al., 2019), which are characterized by an atmosphere with a large variety of anthropogenic pollutants.

In this study, we conducted aerosol measurements using a TD coupled with an Aerodyne high-resolution time-of-flight aerosol mass spectrometer (TD-HR-AMS) and other collocated instruments at a rural site in the NCP region in summer 2013. Besides investigating the sources and volatility of organic aerosol (OA), we also focused on characterizing the particulate ON with mass concentration, volatility and their possible sources in the NCP rural region.

2. Materials and methods

2.1. *Site description and instrumentation*

The sampling site (39.80°N, 116.96°E; 15 m MSL) was at Xianghe Atmospheric Observatory of the Institute of Atmospheric Physics, Chinese Academy of Sciences. This site is a rural site surrounded by agricultural fields and located between Beijing and Tianjin, which are the two most important megacities in the NCP region (Fig. 1). The site's location means that it experiences plumes derived from local agricultural activities or regional transport from urban areas. Measurements were performed from 9 June to 9 July 2013.

The TD-HR-AMS system was deployed at the site to characterize the chemical compositions, mass concentrations and volatility of non-refractory particulate matter (NR-PM_1) (DeCarlo et al., 2006; Canagaratna et al., 2007). A detailed description of the setup and operation of the TD-HR-AMS during measurements can be found in our previous studies (Cao et al., 2018, 2019). Briefly, a $PM_{2.5}$ cyclone was used to remove coarse particles and introduce the ambient air into the TD-HR-AMS and a scanning mobility particle sizer system (3775 CPC and 3080 DMA, TSI Inc.) through a copper tube with a flow of 10 L min^{-1}. The TD was positioned upstream of the HR-ToF-AMS, and the flow rate passing through the TD was 0.45 L min^{-1} with a residence time of ~27.9 s in the heating section. The TD included a heating section and denuder section. The temperatures in the heating section were set at 48°C, 95°C, 143°C and 192°C, corresponding to the measured temperatures of 50°C, 100°C, 150°C and 200°C, respectively. Ambient aero-

sols can pass through directly (bypass flow) or through the TD section (TD flow), and are then dried by a nafion to eliminate the potential influence of relative humidity on the particle collection efficiency (CE) (Matthew et al., 2008). The ionization efficiency (IE) and size calibrations were performed with size-selected pure ammonium-nitrate particles every two weeks. A composition-dependent CE was applied to the data based on the method of Middlebrook et al. (2012). The NR-PM$_1$ species were quantified by the V-mode with unit mass resolution, while the high-resolution mass spectral data were obtained by the W-mode. We operated the HR-ToF-AMS in four menus: bypass flow in V-mode, TD flow in V-mode, TD flow in W-mode, and bypass flow in W-mode, each with a sampling time of 2 min. Besides the TD-HR-AMS system, an aethalometer (AE-31, Magee Inc.) was simultaneously used to measure refractory black carbon (BC) with a temporal resolution of 5 min. The wavelength of 880 nm was used to calculate the mass concentration of BC. The total measured BC can be divided into BC derived from traffic emissions (BC_tr) and biomass burning (BC_bb) based on the aerosol absorption as described in Sandradewi et al., (2008), shown in Text S1 in the Electronic Supplementary Material (ESM).

2.2. *HR-ToF-AMS data routine processing and positive matrix factorization analysis*

The HR-ToF-AMS data routine analysis was performed using the software SQUIRREL (version 1.57) and PIKA (version 1.16) downloaded from the ToF-AMS software downloads webpage (http://cires1.colorado.edu/jimenezgroup/ToFAMSResources/ToFSoftware/index.html) written in Igor Pro 6.37 (Wave Metrics Inc.). The relative IEs for organics, nitrates and chlorides were assumed to be 1.4, 1.1 and 1.3, respectively. A composition-dependent CE was applied to the data based on the method of Middlebrook et al. (2012). Organic elemental analyses, such as the oxygen-to-carbon ratio (O:C), and hydrogen-to-carbon ratio, are determined by the latest procedures proposed by Canagaratna et al. (2015).

Positive matrix factorization (PMF) analysis is a mathematical technique for solving bilinear unmixing problems (Paatero and Tapper, 1994), and has been widely applied in the aerosol community for source apportionment (Lanz et al., 2007; Jimenez et al., 2009; Ulbrich et al., 2009; Huang et al., 2010, 2013; Ng et al., 2010; Xu et al., 2015a, b; Beddows and Harrison, 2019). PMF analysis for AMS data describes the measured matrix as the linear combination of different factors with a constant mass spectrum and their corresponding time series. The observed data matrix and error matrix were generated with the default fragmentation table in PIKA v1.16 and pretreated the error matrix using PMF Evaluation Toolkit software, following the procedure described in Ulbrich et al. (2009). Ions with a signal-to-noise ratio (SNR) less than 0.2 were removed and ions with an SNR ranging between 0.2 and 2 were downweighted by a factor of 2. The ions of H_2O^+, HO^+, O^+, and CO^+, which are related to CO_2^+, were also downweighted since they could introduce additional weight to CO_2^+ (Ulbrich et al., 2009). Then, we performed PMF runs with a range from 1 to 10 factors with FPEAK ("FPEAK" is a tool used to explore rotations of the solutions of a given number of factors) varying from −1 to 1 in steps of 0.1, and SEED ("SEED" is a tool used to choose different random starts for the PMF algorithm) varying from 0 to 250 in steps of 10. The obtained solution of PMF was evaluated carefully according to the procedure outlined in Zhang et al. (2011). According to the diagnostic plots shown in Fig. S1 in the ESM, we found that PMF solutions with factor numbers greater than 4 provided no new distinct meaningful factors and instead split the existing factors. The optimal solution was a 4-factor (FPEAK = 0 and SEED = 0) solution—namely, a hydrocarbon-like OA (HOA), a biomass burning OA (BBOA), a less-oxidized oxygenated OA (LO-OOA), and a more-oxidized oxygenated OA (MO-OOA)—after examining the $Q/Q_{expected}$ value, the residuals of PMF fits, mass spectrum (MS) signatures, their correlation with tracers, diurnal trends, and other characteristics.

2.3. *Estimation of ON mass concentration*

In this study, we used two indirect methods to quantify nitrate functionality of ON mass concentration (i.e., $NO_{3,org}$) based on HR-ToF-AMS measurements. The first method was based on the NO^+/NO_2^+ ratio (denoted as the NO_x^+ ratio hereafter) in the HR-AMS spectrum (Farmer et al., 2010). The NO_x^+ ratio in AMS is significantly higher for ON than ammonium nitrates, according to previous laboratory studies (Fry et al., 2009; Bruns et al., 2010; Farmer et al., 2010; Boyd et al., 2015). Based on this, Farmer et al. (2010) proposed the NO_2 and NO concentrations for ON ($NO_{2,ON}$ and NO_{ON}) can be quantified with the HR-AMS data as follows:

$$NO_{2,ON} = \frac{NO_{2,obs}\left(R_{obs} - R_{NH_4NO_3}\right)}{R_{ON} - R_{NH_4NO_3}}, \qquad (1)$$

$$NO_{ON} = R_{ON}NO_{2,ON}, \qquad (2)$$

where R_{obs} is the NO_x^+ ratio from the observation, $R_{NH_4NO_3}$ is determined by IE calibration using pure ammonium nitrate particles (in this study, the average value of $R_{NH_4NO_3}$ was 2.15 and 2.31 for the first and second IE calibration, respectively), and R_{ON} represents the NO_x^+ ratio for ON, which varies between instruments and precursor volatile organic compounds (VOCs) (Fry et al., 2009; Boyd et al., 2015). Fortunately, $R_{ON}/R_{NH_4NO_3}$ has been assumed to be instrument-independent (Fry et al., 2013). In this study, we adopted an $R_{ON}/R_{NH_4NO_3}$ range from 1.4 to 3.99, which was based on laboratory study results of ON formed from different VOCs (i.e., 1.4 for 3-Methylfuran, 2.08 for isoprene, 2.25 for the organic nitrate standards, 3.99 for β-pinene) (Bruns et al., 2010; Farmer et al., 2010; Sato et al., 2010; Boyd et al., 2015; Joo et al., 2019), to determine R_{ON} in estimating ON.

The second method was based on PMF analysis. We performed the same PMF analysis on HR organic mass spectra

combining NO^+ and NO_2^+ ions to quantify the contributions of ON and ammonium nitrates (Hao et al., 2014; Xu et al., 2015b; Yu et al., 2019). In this method, the NO^+ and NO_2^+ ions were distributed among different OA factors and inorganic aerosol (NIA) factor. Three organic factors (HOA, BBOA and OOA) and one NIA factor were identified using PMF analysis on organic and NO_x^+ fragments (denoted as PMF_{org+NO_x} hereafter). It should be noted that we cannot resolve subtypes of OOA factors from PMF_{org+NO_x} analysis. However, OOA factor from PMF_{org+NO_x} show a good correlation on time series with the sum of LO-OOA and MO-OOA factors from PMF on organic spectra (Fig. S3 in the ESM), suggesting PMF_{org+NO_x} also provided a reasonable result in resolving factors. After determining the optimal solution, the NO^+ and NO_2^+ ions were distributed among different OA factors and the NIA factor. The concentration of $NO_{3,org}$ is equal to the sum of NO^+ and NO_2^+ in the organic nitrates (i.e., NO_{org}^+ and $NO_{2,org}^+$), which are estimated via Eqs. (3) and (4), respectively (Xu et al., 2015b):

$$NO_{org}^+ = \sum ([OA\ factor]_i f_{NOi}), \qquad (3)$$

$$NO_{2,org}^+ = \sum \left([OA\ factor]_i f_{NO2,i}\right), \qquad (4)$$

where $[OA\ factor]_i$ represents the mass concentration of the ith OA factor and f_{NOi} and $f_{NO2,i}$ represent the mass fractions of NO^+ and NO_2^+, respectively.

3. Results and discussion

3.1. *PM₁ composition and OA source apportionment*

The daily average ambient PM_1 mass concentration was 51.2 ± 48.0 μg m⁻³ (mean ± standard deviation), ranging from 1.5 to 466 μg m⁻³, shown in Fig. 2a. The biggest contributor of PM_1 mass loading during summer 2013 was organic (35.4%), followed by sulfate (31.3%), ammonium (12.8%) and nitrate (11.4%) (Fig. 2b). Figure 2c indicates

the variation in relative contributions of different species as a function of the total PM_1 mass loading. We can see that organics show a continuously increasing fraction when PM_1 was accumulating, implying OA played a more important role in extremely polluted periods. Therefore, we discuss the source apportionment of OA further below.

PMF analysis for OA resolved four OA factors: HOA, BBOA, LO-OOA and MO-OOA. The MS profiles and the mass contributions of each factor are shown in Figs. 3a and b. The mass fractions of HOA, BBOA, LO-OOA and MO-OOA were 18.4%, 29.4%, 21.4% and 30.8%, respectively. Note that biomass burning is a large contributor to OA due to the summer wheat harvest in the NCP region. BBOA was found to contribute 36%–39% to OA during harvest seasons in China (Zhang et al., 2015). The characteristics of the mass profile for each factor are distinct. HOA had an MS profile characterized by a large fraction of $C_xH_y^+$ fragments and the lowest O:C ratio of 0.11, as well as the best correlation with BC emitted from traffic (BC_tr) (shown in Fig. S4 in the ESM), indicating its primary nature and high relevance to traffic emissions (Aiken et al., 2009; Huang et al., 2012, 2013; Mohr et al., 2012). The BBOA MS profile contained the highest $f60$ (ratio of the integrated signal at m/z 60 to the total organics signal) value of 0.9% compared to other factors (Schneider et al., 2006; Alfarra et al., 2007; Cubison et al., 2011). BBOA correlated best with acetonitrile (Fig. S4), which is a VOC tracer for biomass burning (Holzinger et al., 1999). However, its O:C ratio reaches up to 0.62. Therefore, BBOA in this case can be regarded as a factor that undergoes chemical aging from fresh emissions, considering the distance between the sampling site and biomass burning fields. Several studies have reported that fresh BBOA could be oxidized rapidly and converted to OOA in less than one day (Bougiatioti et al., 2014; Zhou et al., 2017). The MS profiles of two subtype OOAs were characterized by $C_xH_yO_z^+$ ions, with different fractions of CO_2^+, and have better correlations with sulfate and nitrate (Fig. S4). The diurnal variations of the four OA factors are shown in Fig. 3c. HOA had two pronounced "rush hour" increases in the morning (starting from
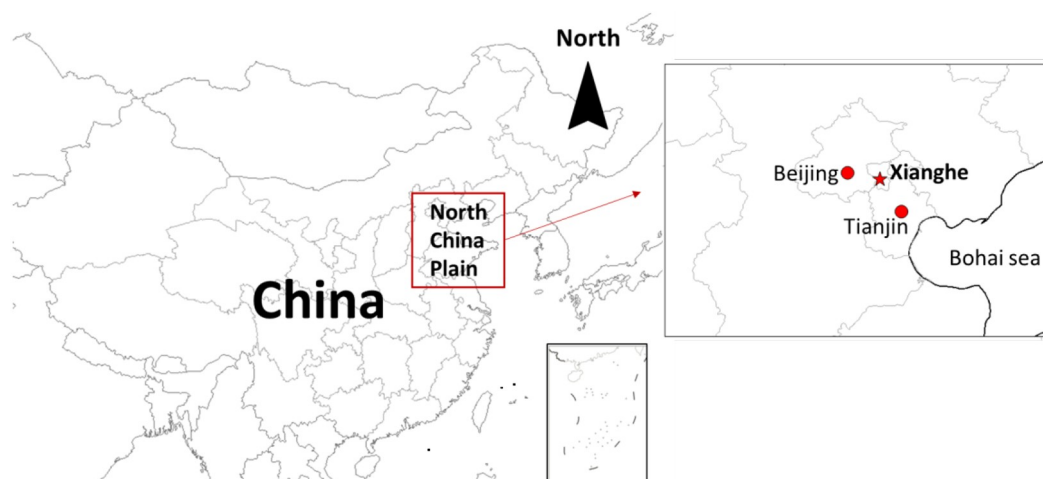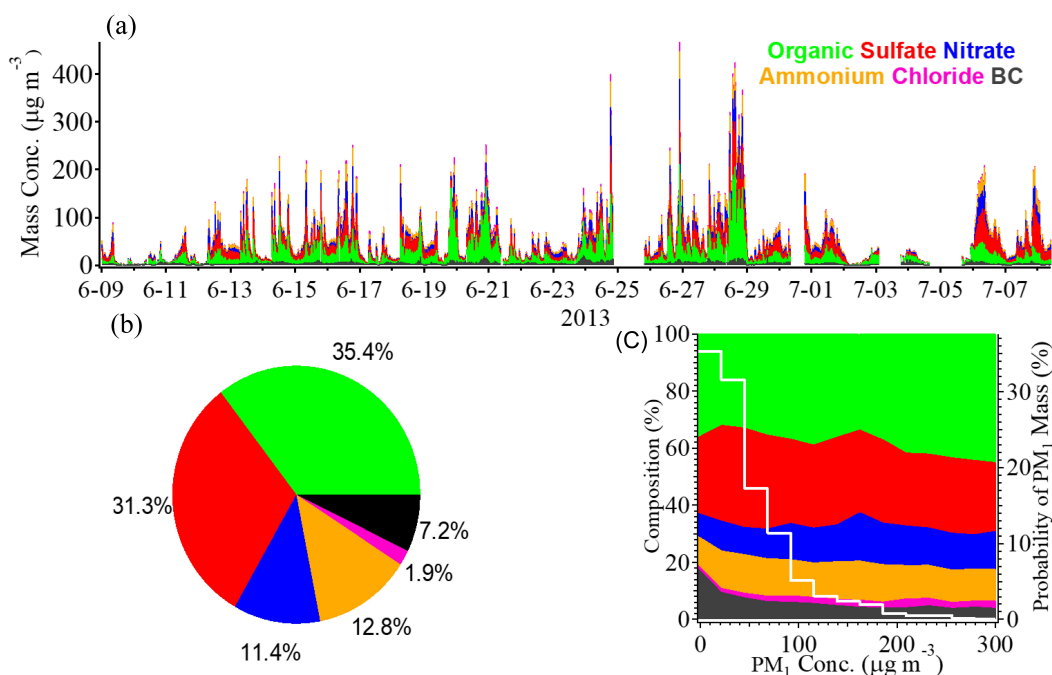

**Fig. 1**. Location of the sampling site (Xianghe).

Fig. 2. (a) Time series of PM_1 species. (b) Pie chart showing the average chemical compositions. (c) Evolutions of PM_1 compositions (left-hand axis) as a function of PM_1 mass concentration, and the probability distributions of PM_1 mass concentration (white line to the right-hand axis).

0700 LST) and in the evening (starting from 1800 LST). The diurnal trend of BBOA had several peaks, which may suggest biomass burning events occurred frequently. LO-OOA and MO-OOA had a similar variation pattern, with an increase starting from 0700 LST and a decrease at 1800 LST, mainly driven by photochemical oxidation accumulation.

3.2. Estimating results of ON and correlation analysis

We first applied the NO_x^+ ratio method to estimate the concentration of nitrate functionality of ON (i.e., $NO_{3,org}$). The concentration of $NO_{3,org}$ and the mass fraction of $NO_{3,org}$ in total measured NO_3 (total NO_3) are shown in Table 1. $NO_{3,org}$ accounted for 7.8% to 12% in NO_3 by using the upper and lower bound values of $R_{ON}/R_{NH_4NO_3}$ in the NO_x^+ ratio method. Then, we used the PMF method to estimate $NO_{3,org}$ to verify the reliability of the results. The MS of the NIA factor is dominated by NO_x^+, and the mass fractions of $NO_x^+>$ in HOA, BBOA, OOA were 11.8%, 85% and 3.2%, respectively (Fig S2). Figure 4a shows the time series of the $NO_{3,org}$ concentration calculated by the two methods and the computed correlation coefficient between them is good ($r = 0.76$), and the slope of the fitting line is 1.2, indicating that similar results were achieved. We further calculated that ON contributed 8.1%–19% to total OA assuming an average molecular weight of ON of 200–300 g mol^{-1} (Rollins et al., 2012), which is comparable to the fraction of ON in OA in Shenzhen during summertime (11%–25%) reported in Yu et al. (2019), indicating ON was the significant component of OA in the rural NCP atmosphere in summer.

Figure 5a shows scatterplots of $NO_{3\_org\_ratio\_1}$ versus OA factors resolved by PMF analysis, BC from biomass burning (BC_bb), and BC from traffic emissions (BC_tr). We find that $NO_{3\_org\_ratio\_1}$ had good correlations with BBOA ($r = 0.71$) and BC_bb ($r = 0.67$), but a poor correlation with LO-OOA ($r = 0.20$), which is quite different from the results in other regions that show the highest ON correlation with LO-OOA (Xu et al., 2015a, b; Yu et al., 2019). Particulate ON formation is found to be through photooxidation of biogenic VOCs in the presence of NO_x in the daytime (Teng et al., 2015, 2017) and NO_3 radicals oxidation of biogenic VOCs at night (Fry et al., 2013; Ayres et al., 2015; Boyd et al., 2015; Xu et al., 2015b; Lee et al., 2016; Yu et al., 2019). However, recent studies show that NO_3 radicals reacting with typical VOCs in biomass burning plumes could also produce a substantial fraction of particulate ON (Ahern et al., 2019; Joo et al., 2019). The good correlation between ON and biomass burning aerosols in this study indicate the possible existence of different formation mechanisms of ON relevant to biomass burning plumes in the real atmosphere. Here, we further compared the diurnal variation of $NO_{3\_org\_ratio}$, inorganic nitrates (NO_{3_inorg}), BBOA and BC_bb in Fig. 4c. First, the result shows that $NO_{3\_org\_ratio}$ had a quite different diurnal variation from NO_{3_inorg}, implying that ON has been well separated from inorganic nitrates in this study. Furthermore, $NO_{3\_org\_ratio}$ increased by nearly two times from 1700 LST to 2200 LST and maintained a relative high mass loading level during the nighttime. We note that there were two similar peaks at 2100–2200 LST and 0300–0400 LST in the $NO_{3\_org\_ratio}$, BBOA and BC_bb variation trends. A number of studies have proposed that night-
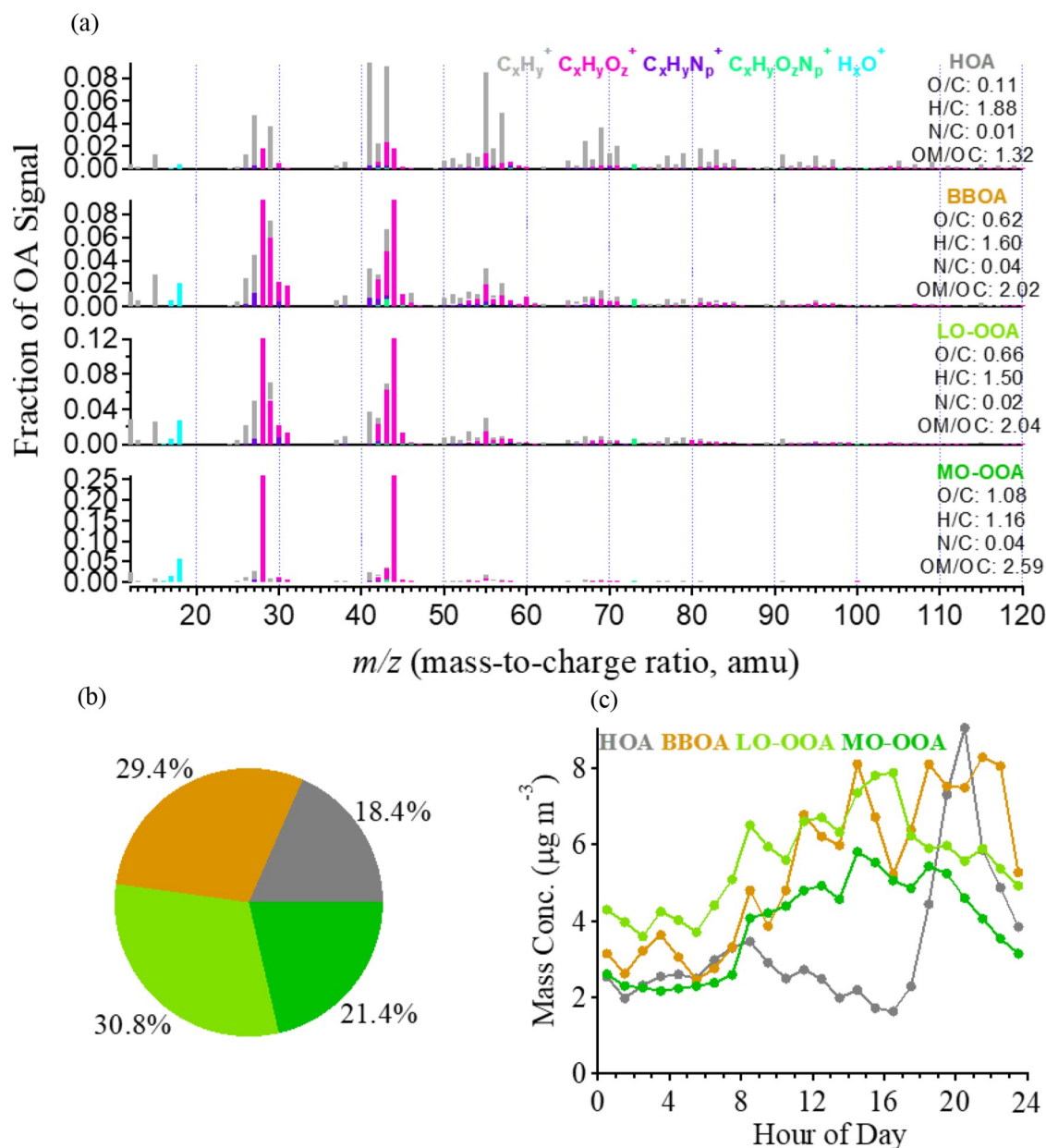
Fig. 3. (a) MS profiles of the OA factors. (b) Pie chart showing the average OA components. (c) Diurnal patterns of the OA components.

**Table 1**. Summary of ON estimations using the NO⁺/NO₂⁺ ratio method and the PMF method.

	Values	
(a) NO⁺/NO₂⁺ ratio method		
	Lower	Upper
$NO_{3,org}$ (µg m⁻³)[a]	0.46	0.70
$NO_{3,org}$/total NO_3	0.078	0.12
(b) PMF method		
$NO_{3,org}$ (µg m⁻³)[b]	0.54	
$NO_{3,org}$/total NO_3	0.093	

Notes: [a]$NO_{3,\,org}$ for upper bound is denoted as $NO_{3\_org\_ratio\_1}$, and $NO_{3,\,org}$ for lower bound is denoted as $NO_{3\_org\_ratio\_2}$; [b]$NO_{3,\,org}$ estimated using the PMF method is denoted as $NO_{3\_org\_PMF}$.

time biomass burning contributes to OA compositions in field campaigns, in particular with some specific ON species formation (Allan et al., 2010; Iinuma et al., 2010, 2016; Mohr et al., 2013). However, these studies did not describe the influence of biomass burning on overall ON. In order to better understand ON in this case, we will attempt to characterize it from the property of volatility in the following section.

3.3. Volatility characteristics of OA factors and ON

The mass fraction remaining (MFR) of different OA factors resolved by PMF analysis, ON and inorganic nitrates are shown in Fig. 6. MFRs varied differently among different OA factors. The MFR of HOA was 0.58 at 50°C and
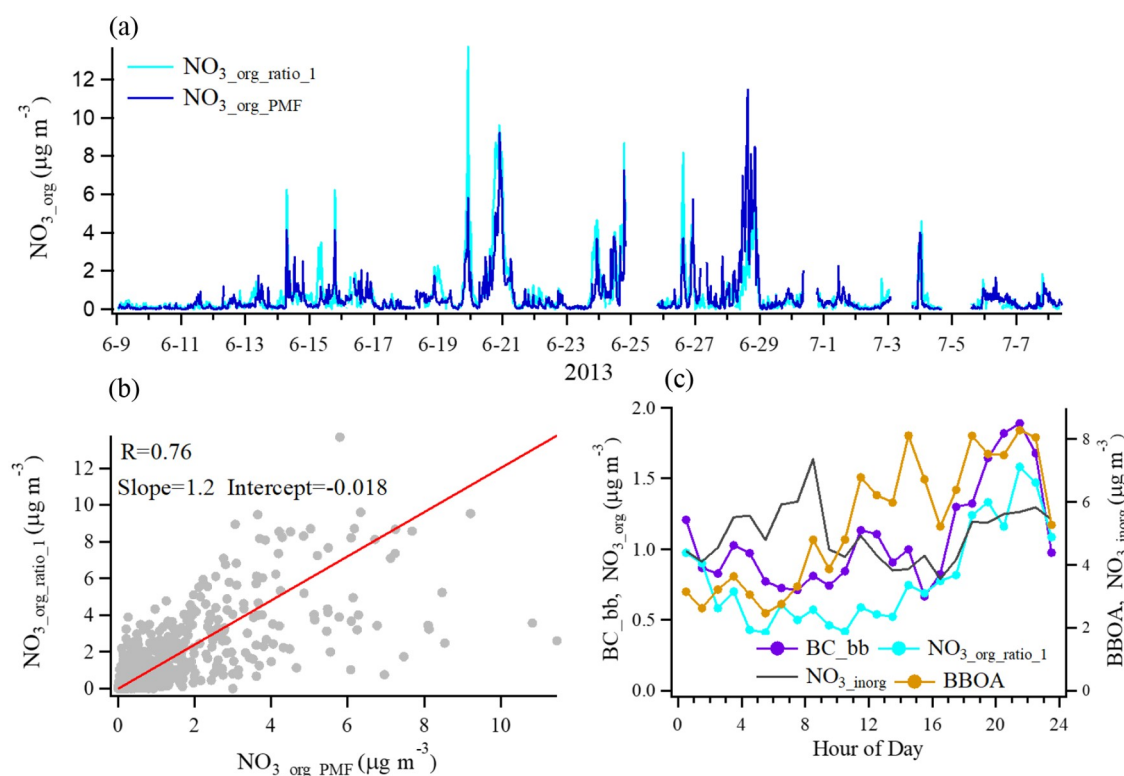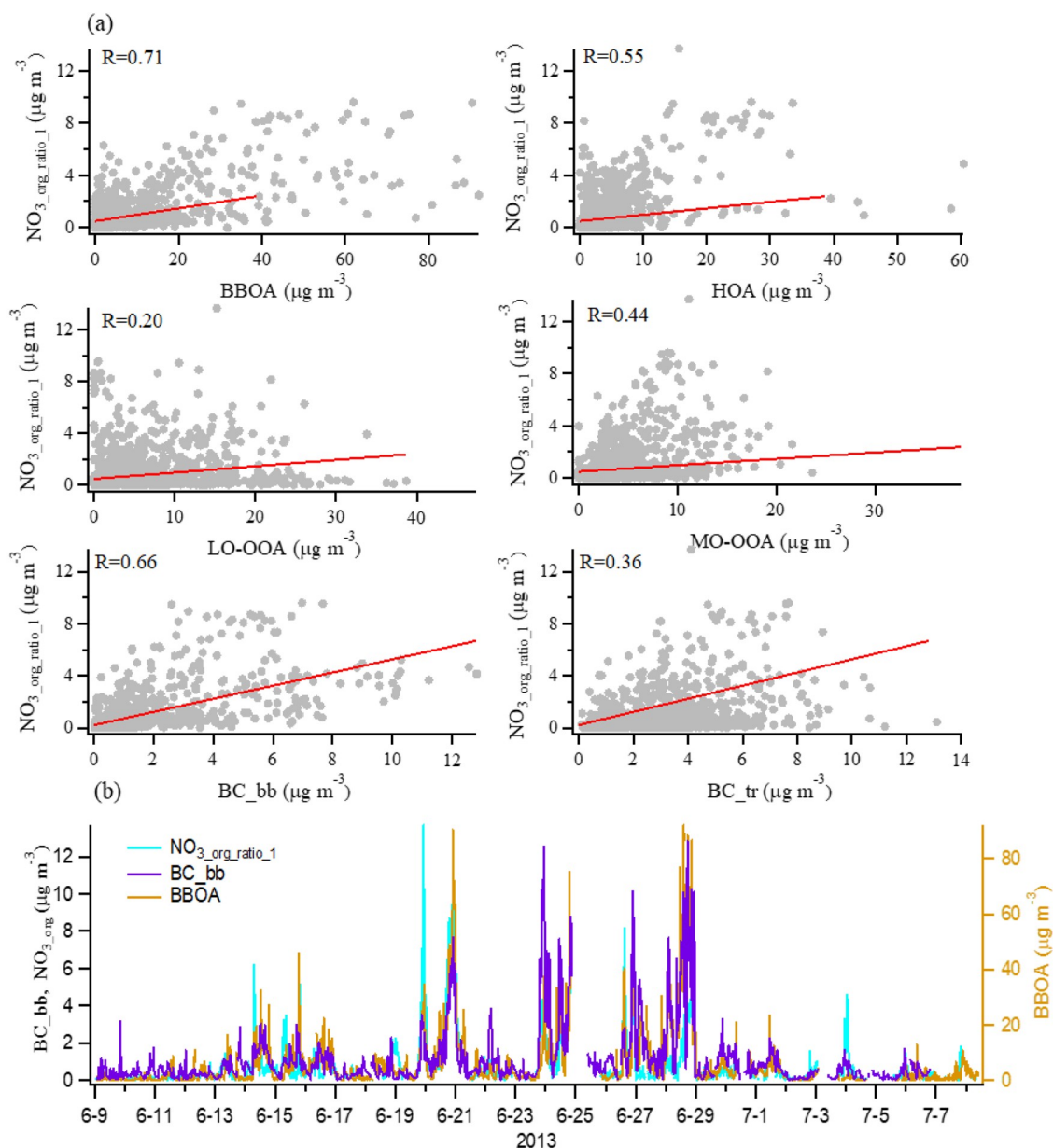
Fig. 4. (a) Time series of $NO_{3,\,org}$ concentration estimated by the NO^+/NO_2^+ ratio method and PMF method for the study period. (b) Correlations between $NO_{3\_org\_ratio\_1}$ and $NO_{3\_org\_PMF}$. (c) Diurnal trends of $NO_{3\_org\_ratio\_1}$, BC_bb (left-hand axis), inorganic nitrates (NO_{3_inorg}) and BBOA (right-hand axis).

decreased by 1.70 % °C⁻¹; then the evaporation rate slowed down from 50°C to 200°C with a nearly constant rate of 0.35% °C⁻¹, and only 4.9% was left at 200°C. BBOA had a similar MFR variation to HOA, with a fast decrease from ambient temperature to 50°C (evaporation rate was 2% °C⁻¹) and a slower decrease from 50°C to 200°C (0.5% °C⁻¹ for 50°C–150°C and 0.006% °C⁻¹ for 150°C–200°C), but much wider standard deviation (SD) areas at temperature stages, suggesting BBOA contained more compounds that have different evaporation, which agrees with the BBOA factor in this case consisting of fresh and aged ones. The MFR of LO-OOA at 50°C was 0.72, lower than that of MO-OOA (0.80) and with increased temperature, and the MFR of MO-OOA decreased much slower than LO-OOA and other OA factors, both implying that MO-OOA was less volatile compared to other OA factors. The volatility sequence of OA factors in this study was HOA > BBOA > LO-OOA > MO-OOA, determined by the MFR at 50°C (Cao et al., 2018, 2019; Xu et al., 2019).

In order to investigate the volatility of ON, we estimated the mass concentration of $NO_{3,org}$ at different temperatures using the NO_x^+ ratio and PMF method as well. Table S1 lists the estimated results and comparison coefficients between the two methods. The good correlation coefficients ($R = 0.68$–0.75) between the two methods validate the ON estimated results. Based on that, the MFR of ON

were further calculated, as shown in Fig. 6f. The MFR of ON was 0.54 at 50°C, 0.37 at 100°C, 0.24 at 150°C, and 0.22 at 200°C. Compared to OA factors, ON evaporate faster from ambient temperature to 50°C (1.86% °C⁻¹), implying a volatile feature for primary emissions. However, ON show a much slower decrease than all OA factors except MO-OOA from 50°C–150°C (0.29% °C⁻¹) and remained flat from 150°C–200°C, suggesting about 20% of the fraction of ON were very difficult to volatilize. In addition, we calculated the MFR for inorganic nitrates, which evaporate much faster than ON and only 4.1% of inorganic nitrates were left at 200°C, confirming the semi-volatility property of inorganic nitrates. Our result provides direct evidence that a considerable remaining fraction of nitrate measured by AMS at high temperature is due to the influence of ON contained within (Cao et al., 2018, 2019; Xu et al., 2019). It should be noted that a laboratory study reported that pure ammonium nitrates can completely evaporate at 50°C (Huffman et al., 2009b), but 35.3% of inorganic nitrates were left at 50°C in our study. The discrepancy may be due to the significant influence of the composition differences and mixing state of ambient aerosols, which has been proposed in previous studies (Huffman et al., 2009b; Nie et al., 2017), and the inaccuracy of the estimation of ON. Therefore, more related studies need to be conducted in the future.

Fig. 5. (a) Correlations of $NO_{3,\,org1\_ratio}$ with OA factors resolved by PMF, BC from biomass burning (BC_bb), and BC from traffic emissions (BC_tr). (b) Time series of $NO_{3,\,org}$ concentration estimated by the NO^+/NO_2^+ ratio method (NO_{3_org}), BC_bb (left axis) and BBOA (right-hand axis).

4. Conclusions

In this study, we characterized submicron aerosols based on TD-HR-AMS measurements at a rural site in NCP during summer 2013. The mean PM_1 mass loading was 51.2 ± 48.0 μg m^{-3}, with organics as the most abundant species. Sulfate, ammonium, nitrate, BC and chloride contributed 31.3%, 12.8%, 11.4%, 7.2% and 1.9% to the total PM_1, respectively. PMF analysis of OA identified four OA factors: HOA, BBOA, LO-OOA and MO-OOA. Among them, two subtype OOAs accounted for 52.2% of OA, and BBOA also made a substantial contribution (29.4%) to OA. In terms of volatility, HOA was the most volatile species (MFR was 0.58 at 50°C), followed by BBOA (0.62), LO-

OOA (0.72) and MO-OOA (0.80).

The ON were quantified by two methods, i.e., NO_x^+ ratio method and PMF method. Both methods provided reasonable and comparable results in abstracting ON functionality from total measured nitrates. The nitrate functionality of ON (i.e., $NO_{3,org}$) accounted for about 7.8%–12% of total measured nitrates (NO_3). Furthermore, the mass concentration of ON was estimated assuming the molecular weight of bulk ON, and they contributed a substantial fraction (8.1%–19%) to total OA. ON show good correlations with BBOA ($r = 0.71$) and BC from biomass burning ($r = 0.67$) but poor correlation with LO-OOA ($r = 0.20$). High levels of biomass burning emissions at night and several similar nighttime peaks of ON, BBOA and BC from biomass burn-
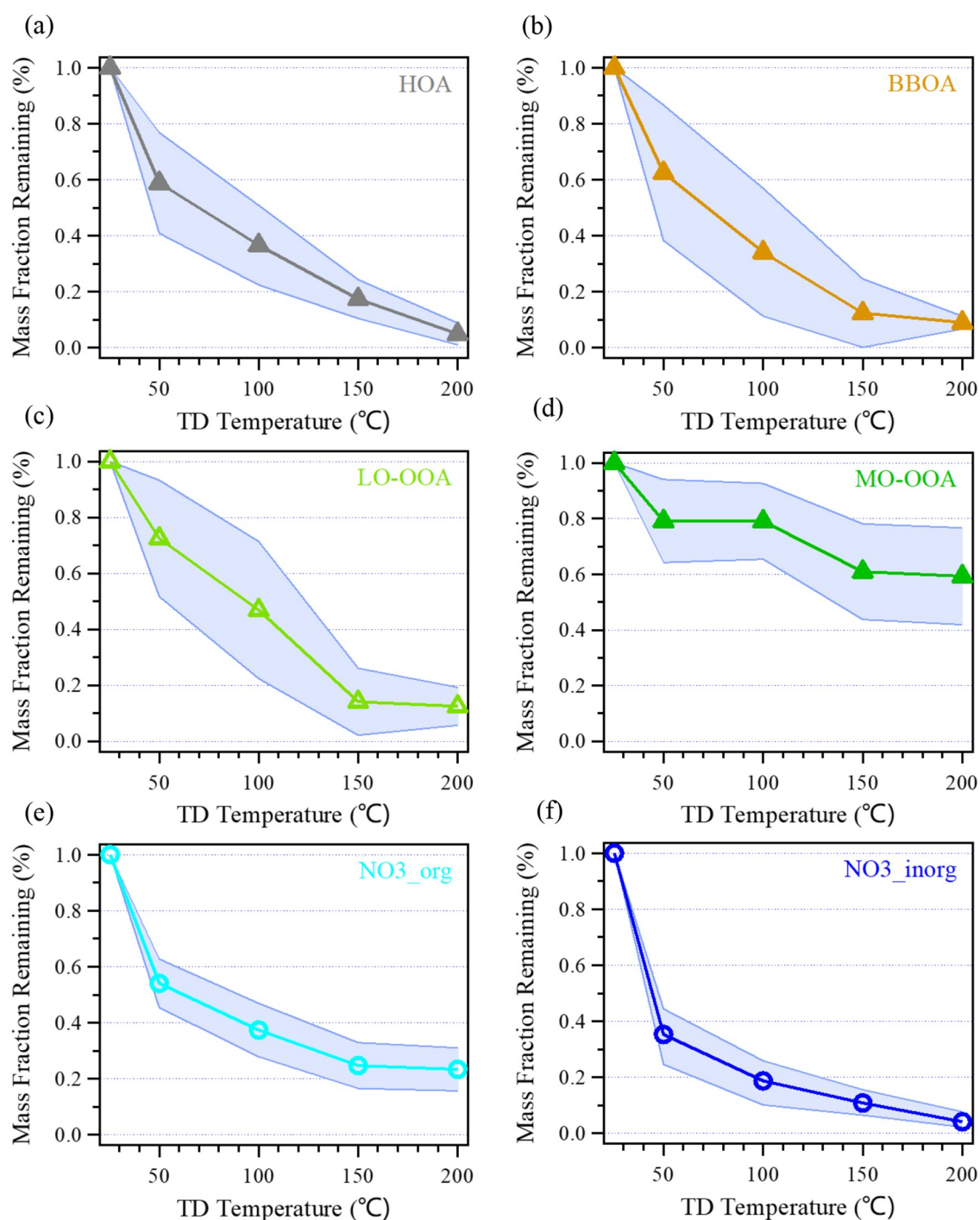
Fig. 6. Variation of the average MFR of OA factors (a–d) resolved by PMF, ON (NO_{3_org}) (e), and inorganic nitrates (f) with the TD temperature. The shaded regions indicate the average ± SD.

ing in diurnal trends suggest ON were influenced by biomass burning. The volatility analysis shows that the overall ON were more volatile than other OA factors at 50°C. Based on these results, we can conclude that particulate ON in rural NCP areas are more relevant to primary emissions, with biomass burning as the most likely source responsible.

REFERENCES

Aiken, A. C., and Coauthors, 2009: Mexico City aerosol analysis during MILAGRO using high resolution aerosol mass spectrometry at the urban supersite (T0)−Part 1: Fine particle composition and organic source apportionment. *Atmospheric Chemistry and Physics*, **9**, 6633−6653, https://doi.org/10.5194/acp-9-6633-2009.

Ahern, A. T., and Coauthors, 2019: Production of secondary organic aerosol during aging of biomass burning smoke from fresh fuels and its relationship to VOC precursors. *J. Geophys. Res.*, **124**, 3583−3606, https://doi.org/10.1029/2018JD029068.

Alfarra, M. R., and Coauthors, 2007: Identification of the mass spectral signature of organic aerosols from wood burning emissions. *Environ. Sci. Technol.*, **41**, 5770−5777, https://doi.org/10.1021/es062289b.

Allan, J. D., and Coauthors, 2010: Contributions from transport, solid fuel burning and cooking to primary organic aerosols in two UK cities. *Atmospheric Chemistry and Physics*, **10**, 647−668, https://doi.org/10.5194/acp-10-647-2010.

Ayres, B. R., and Coauthors, 2015: Organic nitrate aerosol formation via NO_3^+ biogenic volatile organic compounds in the southeastern United States. *Atmospheric Chemistry and Physics*, **15**, 13377−13392, https://doi.org/10.5194/acp-15-13377-2015.

Beddows, D. C. S., and R. M. Harrison, 2019: Receptor modelling of both particle composition and size distribution from a background site in London, UK−A two-step approach. *Atmospheric Chemistry and Physics*, **19**, 4863−4876, https://doi.org/10.5194/acp-19-4863-2019.

Bertman, S. B., and Coauthors, 1995: Evolution of alkyl nitrates with air mass age. *J. Geophys. Res.*, **100**, 22805−22813, https://doi.org/10.1029/95JD02030.

Bi, X. H., and Coauthors, 2015: Real-time and single-particle volatility of elemental carbon-containing particles in the urban area of Pearl River Delta region, China. *Atmos. Environ.*, **118**, 194−202, https://doi.org/10.1016/j.atmosenv.2015.08.012.

Bilde, M., and Coauthors, 2015: Saturation vapor pressures and transition enthalpies of low-volatility organic molecules of atmospheric relevance: From dicarboxylic acids to complex mixtures. *Chemical Reviews*, **115**, 4115−4156, https://doi.org/10.1021/cr5005502.

Bougiatioti, A., and Coauthors, 2014: Processing of biomass-burning aerosol in the eastern Mediterranean during summertime. *Atmospheric Chemistry and Physics*, **14**, 4793−4807, https://doi.org/10.5194/acp-14-4793-2014.

Boyd, C. M., J. Sanchez, L. Xu, A. J. Eugene, T. Nah, W. Y. Tuet, M. I. Guzman, and N. L. Ng, 2015: Secondary organic aerosol formation from the β-pinene+NO_3 system: Effect of humidity and peroxy radical fate. *Atmospheric Chemistry and Physics*, **15**, 7497−7522, https://doi.org/10.5194/acp-15-7497-2015.

Boyd, C. M., T. Nah, L. Xu, T. Berkemeier, and N. L. Ng, 2017: Secondary Organic Aerosol (SOA) from nitrate radical oxidation of monoterpenes: Effects of temperature, dilution, and humidity on aerosol formation, mixing, and evaporation. *Environ. Sci. Technol.*, **51**, 7831−7841, https://doi.org/10.1021/acs.est.7b01460.

Bruns, E. A., and Coauthors, 2010: Comparison of FTIR and particle mass spectrometry for the measurement of particulate organic nitrates. *Environ. Sci. Technol.*, **44**, 1056−1061, https://doi.org/10.1021/es9029864.

Canagaratna, M. R., and Coauthors, 2007: Chemical and microphysical characterization of ambient aerosols with the aerodyne aerosol mass spectrometer. *Mass Spectrometry Reviews*, **26**, 185−222, https://doi.org/10.1002/mas.20115.

Canagaratna, M. R., and Coauthors, 2015: Elemental ratio measurements of organic compounds using aerosol mass spectrometry: Characterization, improved calibration, and implications. *Atmospheric Chemistry and Physics*, **15**, 253−272, https://doi.org/10.5194/acp-15-253-2015.

Cao, L.-M., X.-F. Huang, Y.-Y. Li, M. Hu, and L.-Y. He, 2018: Volatility measurement of atmospheric submicron aerosols in an urban atmosphere in southern China. *Atmospheric Chemistry and Physics*, **18**, 1729−1743, https://doi.org/10.5194/acp-18-1729-2018.

Cao, L.-M., X.-F. Huang, C. Wang, Q. Zhu, and L.-Y. He, 2019: Characterization of submicron aerosol volatility in the regional atmosphere in Southern China. *Chemosphere*, **236**, 124383, https://doi.org/10.1016/j.chemosphere.2019.124383.

Charlson, R. J., and J. Heintzenberg, 1995: *Aerosol Forcing of Climate*. Wiley, Chichester, 184-195.

Cubison, M. J., and Coauthors, 2011: Effects of aging on organic aerosol from open biomass burning smoke in aircraft and laboratory studies. *Atmospheric Chemistry and Physics*, **11**, 12049−12064, https://doi.org/10.5194/acp-11-12049-2011.

Dassios, K. G., and S. N. Pandis, 1999: The mass accommodation coefficient of ammonium nitrate aerosol. *Atmos. Environ.*, **33**, 2993−3003, https://doi.org/10.1016/S1352-2310(99)00079-5.

DeCarlo, P. F., and Coauthors, 2006: Field-deployable, high-resolution, time-of-flight aerosol mass spectrometer. *Analytical Chemistry*, **78**, 8281−8289, https://doi.org/10.1021/ac061249n.

Dockery, D. W., C. A. Pope, X. P. Xu, J. D. Spengler, J. H. Ware, M. E. Fay, B. G. Ferris Jr., and F. E. Speizer, 1993: An association between air pollution and mortality in six US cities. *The New England Journal of Medicine*, **329**, 1753−1759, https://doi.org/10.1056/NEJM199312093292401.

Farmer, D. K., A. Matsunaga, K. S. Docherty, J. D. Surratt, J. H. Seinfeld, P. J. Ziemann, and J. L. Jimenez, 2010: Response of an aerosol mass spectrometer to organonitrates and organosulfates and implications for atmospheric chemistry. *Proceedings of the National Academy of Sciences of the United States of America*, **107**, 6670−6675, https://doi.org/10.1073/pnas.0912340107.

Fry, J. L., and Coauthors, 2009: Organic nitrate and secondary organic aerosol yield from NO_3 oxidation of β-pinene evaluated using a gas-phase kinetics/aerosol partitioning model. *Atmospheric Chemistry and Physics*, **9**, 1431−1449, https://doi.org/10.5194/acp-9-1431-2009.

Fry, J. L., and Coauthors, 2013: Observations of gas- and aerosol-phase organic nitrates at BEACHON-RoMBAS 2011. *Atmospheric Chemistry and Physics*, **13**, 8585−8605, https://doi.org/10.5194/acp-13-8585-2013.

Gu, J. X., Z. P. Bai, A. X. Liu, L. P. Wu, Y. Y. Xie, W. F. Li, H. Y. Dong, and X. Zhang, 2010: Characterization of atmospheric organic carbon and element carbon of $PM_{2.5}$ and PM_{10} at Tianjin, China. *Aerosol and Air Quality Research*, **10**, 167−176, https://doi.org/10.4209/aaqr.2009.12.0080.

Hao, L. Q., and Coauthors, 2014: Atmospheric submicron aerosol composition and particulate organic nitrate formation in

a boreal forestland-urban mixed region. *Atmospheric Chemistry and Physics*, **14**, 17263−17298, https://doi.org/10.5194/acp-14-13483-2014.

Haywood, J., and O. Boucher, 2000: Estimates of the direct and indirect radiative forcing due to tropospheric aerosols: A review. *Rev. Geophys.*, **38**, 513−543, https://doi.org/10.1029/1999RG000078.

Holzinger, R., C. Warneke, A. Hansel, A. Jordan, W. Lindinger, D. H. Scharffe, G. Schade, and P. J. Crutzen, 1999: Biomass burning as a source of formaldehyde, acetaldehyde, methanol, acetone, acetonitrile, and hydrogen cyanide. *Geophys. Res. Lett.*, **26**, 1161−1164, https://doi.org/10.1029/1999GL900156.

Huang, X.-F., and Coauthors, 2010: Highly time-resolved chemical characterization of atmospheric submicron particles during 2008 Beijing olympic games using an aerodyne high-resolution aerosol mass spectrometer. *Atmospheric Chemistry and Physics*, **10**, 8933−8945, https://doi.org/10.5194/acp-10-8933-2010.

Huang, X.-F., L.-Y. He, L. Xue, T.-L. Sun, L.-W. Zeng, Z.-H. Gong, M. Hu, and T. Zhu, 2012: Highly time-resolved chemical characterization of atmospheric fine particles during 2010 Shanghai World Expo. *Atmospheric Chemistry and Physics*, **12**, 4897−4907, https://doi.org/10.5194/acp-12-4897-2012.

Huang, X.-F., and Coauthors, 2013: Highly time-resolved carbonaceous aerosol characterization in Yangtze River Delta of China: Composition, mixing state and secondary formation. *Atmos. Environ.*, **64**, 200−207, https://doi.org/10.1016/j.atmosenv.2012.09.059.

Huffman, J. A., P. J. Ziemann, J. T. Jayne, D. R. Worsnop, and J. L. Jimenez, 2008: Development and characterization of a fast-stepping/scanning thermodenuder for chemically-resolved aerosol volatility measurements. *Aerosol Science and Technology*, **42**, 395−407, https://doi.org/10.1080/02786820802104981.

Huffman, J. A., K. S. Docherty, C. Mohr, M. J. Cubison, I. M. Ulbrich, P. J. Ziemann, T. B. Onasch, and J. L. Jimenez, 2009a: Chemically-resolved volatility measurements of organic aerosol from different sources. *Environ. Sci. Technol.*, **43**, 5351−5357, https://doi.org/10.1021/es803539d.

Huffman, J. A., and Coauthors, 2009b: Chemically-resolved aerosol volatility measurements from two megacity field studies. *Atmospheric Chemistry and Physics*, **9**, 7161−7182, https://doi.org/10.5194/acp-9-7161-2009.

Iinuma, Y., O. Böge, R. Gräfe, and H. Herrmann, 2010: Methylnitrocatechols: Atmospheric tracer compounds for biomass burning secondary organic aerosols. *Environ. Sci. Technol.*, **44**, 8453−8459, https://doi.org/10.1021/es102938a.

Iinuma, Y., M. Keywood, and H. Herrmann, 2016: Characterization of primary and secondary organic aerosols in Melbourne airshed: The influence of biogenic emissions, wood smoke and bushfires. *Atmos. Environ.*, **130**, 54−63, https://doi.org/10.1016/j.atmosenv.2015.12.014.

IPCC, 2013: Climate change 2013: The physical science basis. *Contribution of Working Group I to the Fifth Assessment Report of the Intergovernmental Panel on Climate Change*, T. F. Stocker et al., Eds., Cambridge University Press, 1535 pp.

Jenkin, M. E., and K. C. Clemitshaw, 2000: Ozone and other secondary photochemical pollutants: Chemical processes governing their formation in the planetary boundary layer. *Atmos. Environ.*, **34**, 2499−2527, https://doi.org/10.1016/S1352-2310(99)00478-1.

Jimenez, J. L., and Coauthors, 2009: Evolution of organic aerosols in the atmosphere. *Science*, **326**, 1525−1529, https://doi.org/10.1126/science.1180353.

Joo, T., J. C. Rivera-Rios, M. Takeuchi, M. J. Alvarado, and N. L. Ng, 2019: Secondary organic aerosol formation from reaction of 3-methylfuran with nitrate radicals. *ACS Earth and Space Chemistry*, **3**, 922−934, https://doi.org/10.1021/acsearthspacechem.9b00068.

Kolesar, K. R., Z. Y. Li, K. R. Wilson, and C. D. Cappa, 2015: Heating-induced evaporation of nine different secondary organic aerosol types. *Environ. Sci. Technol.*, **49**, 12242−12252, https://doi.org/10.1021/acs.est.5b03038.

Kuhn, T., M. Krudysz, Y. F. Zhu, P. M. Fine, W. C. Hinds, J. Froines, and C. Sioutas, 2005: Volatility of indoor and outdoor ultrafine particulate matter near a freeway. *Journal of Aerosol Science*, **36**, 291−302, https://doi.org/10.1016/j.jaerosci.2004.09.006.

Lanz, V. A., M. R. Alfarra, U. Baltensperger, B. Buchmann, C. Hueglin, and A. S. H. Prévôt, 2007: Source apportionment of submicron organic aerosols at an urban site by factor analytical modelling of aerosol mass spectra. *Atmospheric Chemistry and Physics*, **7**, 1503−1522, https://doi.org/10.5194/acp-7-1503-2007.

Lazaridis, M., 1999: Gas-particle partitioning of organic compounds in the atmosphere. *Journal of Aerosol Science*, **30**, 1165−1170, https://doi.org/10.1016/S0021-8502(98)00788-5.

Lee, B. H., and Coauthors, 2016: Highly functionalized organic nitrates in the southeast United States: Contribution to secondary organic aerosol and reactive nitrogen budgets. *Proceedings of the National Academy of Sciences of the United States of America*, **113**, 1516−1521, https://doi.org/10.1073/pnas.1508108113.

Li, H. Y., and Coauthors, 2017: Wintertime aerosol chemistry and haze evolution in an extremely polluted city of the North China Plain: Significant contribution from coal and biomass combustion. *Atmospheric Chemistry and Physics*, **17**, 4751−4768, https://doi.org/10.5194/acp-17-4751-2017.

Liu, Q., Y. Sun, B. Hu, Z. R. Liu, S. Akio, and Y. S. Wang, 2012: *In situ* measurement of PM1 organic aerosol in Beijing winter using a high-resolution aerosol mass spectrometer. *Chinese Science Bulletin*, **57**, 819−826, https://doi.org/10.1007/s11434-011-4886-0.

Matthew, B. M., A. M. Middlebrook, and T. B. Onasch, 2008: Collection efficiencies in an aerodyne aerosol mass spectrometer as a function of particle phase for laboratory generated aerosols. *Aerosol Science and Technology*, **42**, 884−898, https://doi.org/10.1080/02786820802356797.

Middlebrook, A. M., R. Bahreini, J. L. Jimenez, and M. R. Canagaratna, 2012: Evaluation of composition-dependent collection efficiencies for the aerodyne aerosol mass spectrometer using field data. *Aerosol Science and Technology*, **46**, 258−271, https://doi.org/10.1080/02786826.2011.620041.

Mohr, C., and Coauthors, 2012: Identification and quantification of organic aerosol from cooking and other sources in Barcelona using aerosol mass spectrometer data. *Atmospheric Chemistry and Physics*, **12**, 1649−1665, https://doi.org/10.5194/acp-12-1649-2012.

Mohr, C., and Coauthors, 2013: Contribution of nitrated phenols to wood burning brown carbon light absorption in Detling, United kingdom during winter time. *Environ. Sci. Technol.*,

47, 6316–6324, https://doi.org/10.1021/es400683v.

Ng, N. L., and Coauthors, 2010: Organic aerosol components observed in northern hemispheric datasets from aerosol mass spectrometry. *Atmospheric Chemistry and Physics*, **10**, 4625–4641, https://doi.org/10.5194/acp-10-4625-2010.

Ng, N. L., and Coauthors, 2017: Nitrate radicals and biogenic volatile organic compounds: Oxidation, mechanisms, and organic aerosol. *Atmospheric Chemistry and Physics*, **17**, 2103–2162, https://doi.org/10.5194/acp-17-2103-2017.

Nie, W., and Coauthors, 2017: Volatility of mixed atmospheric humic-like substances and ammonium sulfate particles. *Atmospheric Chemistry and Physics*, **17**, 3659–3672, https://doi.org/10.5194/acp-17-3659-2017.

Paatero, P., and U. Tapper, 1994: Positive matrix factorization: A non-negative factor model with optimal utilization of error estimates of data values. *Environmetrics*, **5**, 111–126, https://doi.org/10.1002/env.3170050203.

Pankow, J. F., and K. C. Barsanti, 2009: The carbon number-polarity grid: A means to manage the complexity of the mix of organic compounds when modeling atmospheric organic particulate matter. *Atmos. Environ.*, **43**, 2829–2835, https://doi.org/10.1016/j.atmosenv.2008.12.050.

Perring, A. E., S. E. Pusede, and R. C. Cohen, 2013: An observational perspective on the atmospheric impacts of alkyl and multifunctional nitrates on ozone and secondary organic aerosol. *Chemical Reviews*, **113**, 5848–5870, https://doi.org/10.1021/cr300520x.

Ramanathan, V., P. J. Crutzen, J. T. Kiehl, and D. Rosenfeld, 2001: Aerosols, climate, and the hydrological cycle. *Science*, **294**, 2119–2124, https://doi.org/10.1126/science.1064034.

Rollins, A. W., and Coauthors, 2012: Evidence for NO_x control over nighttime SOA formation. *Science*, **337**, 1210–1212, https://doi.org/10.1126/science.1221520.

Russo, R. S., Y. Zhou, K. B. Haase, O. W. Wingenter, E. K. Frinak, H. Mao, R. W. Talbot, and B. C. Sive, 2010: Temporal variability, sources, and sinks of C_1-C_5 alkyl nitrates in coastal New England. *Atmospheric Chemistry and Physics*, **10**, 1865–1883, https://doi.org/10.5194/acp-10-1865-2010.

Saha, P. K., and A. P. Grieshop, 2016: Exploring divergent volatility properties from yield and thermodenuder measurements of secondary organic aerosol from α-pinene ozonolysis. *Environ. Sci. Technol.*, **50**, 5740–5749, https://doi.org/10.1021/acs.est.6b00303.

Saleh, R., J. Walker, and A. Khlystov, 2008: Determination of saturation pressure and enthalpy of vaporization of semi-volatile aerosols: The integrated volume method. *Journal of Aerosol Science*, **39**, 876–887, https://doi.org/10.1016/j.jaerosci.2008.06.004.

Sandradewi, J., A. S. H. Prévôt, S. Szidat, N. Perron, M. R. Alfarra, V. A. Lanz, E. Weingartner, and U. Baltensperger, 2008: Using aerosol light absorption measurements for the quantitative determination of wood burning and traffic emission contributions to particulate matter. *Environ. Sci. Technol.*, **42**, 3316–3323, https://doi.org/10.1021/es702253m.

Sato, K., A. Takami, T. Isozaki, T. Hikida, A. Shimono, and T. Imamura, 2010: Mass spectrometric study of secondary organic aerosol formed from the photo-oxidation of aromatic hydrocarbons. *Atmos. Environ.*, **44**, 1080–1087, https://doi.org/10.1016/j.atmosenv.2009.12.013.

Schneider, J., and Coauthors, 2006: Mass spectrometric analysis and aerodynamic properties of various types of combustion-related aerosol particles. *International Journal of Mass Spectrometry*, **258**, 37–49, https://doi.org/10.1016/j.ijms.2006.07.008.

Shrivastava, M. K., E. M. Lipsky, C. O. Stanier, and A. L. Robinson, 2006: Modeling semivolatile organic aerosol mass emissions from combustion systems. *Environ. Sci. Technol.*, **40**, 2671–2677, https://doi.org/10.1021/es0522231.

Song, Y., Y. H. Zhang, S. D. Xie, L. M. Zeng, M. Zheng, L. G. Salmon, M. Shao, and S. Slanina, 2006: Source apportionment of $PM_{2.5}$ in Beijing by positive matrix factorization. *Atmos. Environ.*, **40**, 1526–1537, https://doi.org/10.1016/j.atmosenv.2005.10.039.

Sun, Y. L., Z. F. Wang, H. B. Dong, T. Yang, J. Li, X. L. Pan, P. Chen, and J. T. Jayne, 2012: Characterization of summer organic and inorganic aerosols in Beijing, China with an Aerosol Chemical Speciation Monitor. *Atmos. Environ.*, **51**, 250–259, https://doi.org/10.1016/j.atmosenv.2012.01.013.

Teng, A. P., J. D. Crounse, L. Lee, J. M. St. Clair, R. C. Cohen, and P. O. Wennberg, 2015: Hydroxy nitrate production in the OH-initiated oxidation of alkenes. *Atmospheric Chemistry and Physics*, **15**, 4297–4316, https://doi.org/10.5194/acp-15-4297-2015.

Teng, A. P., J. D. Crounse, and P. O. Wennberg, 2017: Isoprene peroxy radical dynamics. *Journal of the American Chemical Society*, **139**, 5367–5377, https://doi.org/10.1021/jacs.6b12838.

Ulbrich, I. M., M. R. Canagaratna, Q. Zhang, D. R. Worsnop, and J. L. Jimenez, 2009: Interpretation of organic components from Positive Matrix Factorization of aerosol mass spectrometric data. *Atmospheric Chemistry and Physics*, **9**, 2891–2918, https://doi.org/10.5194/acp-9-2891-2009.

Wang, L. T., Z. Wei, J. Yang, Y. Zhang, F. F. Zhang, J. Su, C. C. Meng, and Q. Zhang, 2014: The 2013 severe haze over southern Hebei, China: Model evaluation, source apportionment, and policy implications. *Atmospheric Chemistry and Physics*, **14**, 3151–3173, https://doi.org/10.5194/acp-14-3151-2014.

Xu, L., S. Suresh, H. Guo, R. J. Weber, and N. L. Ng, 2015a: Aerosol characterization over the southeastern United States using high-resolution aerosol mass spectrometry: Spatial and seasonal variation of aerosol composition and sources with a focus on organic nitrates. *Atmospheric Chemistry and Physics*, **15**, 7307–7336, https://doi.org/10.5194/acp-15-7307-2015.

Xu, L., and Coauthors, 2015b: Effects of anthropogenic emissions on aerosol formation from isoprene and monoterpenes in the southeastern United States. *Proceedings of the National Academy of Sciences of the United States of America*, **112**, 37–42, https://doi.org/10.1073/pnas.1417609112.

Xu, W. Q., and Coauthors, 2017: Seasonal characterization of organic nitrogen in atmospheric aerosols using high resolution aerosol mass spectrometry in Beijing, China. *ACS Earth and Space Chemistry*, **1**, 673–682, https://doi.org/10.1021/acsearthspacechem.7b00106.

Xu, W. Q., and Coauthors, 2019: Summertime aerosol volatility measurements in Beijing, China. *Atmospheric Chemistry and Physics*, **19**, 10205–10216, https://doi.org/10.5194/acp-19-10205-2019.

Yu, K. Y., Q. Zhu, K. Du, and X.-F. Huang, 2019: Characterization of nighttime formation of particulate organic nitrates based on high-resolution aerosol mass spectrometry in an urban atmosphere in China. *Atmospheric Chemistry and Phys-*

ics, **19**, 5235−5249, https://doi.org/10.5194/acp-19-5235-2019.

Zhang, Q., J. L. Jimenez, M. R. Canagaratna, I. M. Ulbrich, N. L. Ng, D. R. Worsnop, and Y. L. Sun, 2011: Understanding atmospheric organic aerosols via factor analysis of aerosol mass spectrometry: A review. *Analytical and Bioanalytical Chemistry*, **401**, 3045−3067, https://doi.org/10.1007/s00216-011-5355-y.

Zhang, Y. J., and Coauthors., 2015: Insights into characteristics, sources, and evolution of submicron aerosols during harvest seasons in the Yangtze River delta region, China. *Atmospheric Chemistry and Physics*, **15**, 1331−1349, https://doi.org/10.5194/acp-15-1331-2015.

Zhou, S., and Coauthors, 2017: Regional influence of wildfires on aerosol chemistry in the western US and insights into atmospheric aging of biomass burning organic aerosol. *Atmospheric Chemistry and Physics*, **17**, 2477−2493, https://doi.org/10.5194/acp-17-2477-2017.